Deep–Sea Research II 230 (2026) 105718

Contents lists available at ScienceDirect

Deep-Sea Research Part II

journal homepage: www.elsevier.com/locate/dsr2

Archaea microbiota dynamics and interactions in deep-sea wood fall in the South China sea: insight into the driving patterns of diversity center, community assembly, and biogeochemical processes

Biao Chen [a], Xinrui Zhang [a], Kefu Yu [a,b,*], Zeming Bao [a], Xinyue Liang [a], Xuanlin Li [a], Lin Liang [a], Qicheng Wu [a], He Li [a], Lijia Xu [c]

[a] Guangxi Laboratory on the Study of Coral Reefs in the South China Sea; Coral Reef Research Center of China; School of Marine Sciences, Guangxi University, Nanning, China
[b] Southern Marine Science and Engineering Guangdong Laboratory (Zhuhai), Zhuhai, China
[c] South China Institute of Environmental Sciences, Ministry of Ecology and Environment, Guangzhou, China

ARTICLE INFO

Keywords:
Deep-sea
Wood fall
Archaea microbiota
Community dynamic
Community assembly
Ecological function
South China sea

ABSTRACT

Microbiota are pivotal to the ecological and biogeochemical processes of deep-sea wood-fall ecosystems. However, the dynamics and interactions of archaea within these ecosystems remain poorly understood. This study determined the age and source of a deep-sea wood fall in the South China Sea (SCS) and investigated the diversity, community assembly, and ecological functions of archaeal microbiota via 16S rRNA gene amplicon sequencing. The results showed that the deep-sea wood fall was identified as *Homalium hainanense* Gagnep., with associations to wooden vessels from the 1979-1981 period onwards. The center of taxonomic and functional diversity of the archaeal microbiota is located in the transition region (TR) of the deep-sea wood fall. Compared to the sediment contact surface (SDCS) and seawater contact surface (SWCS), the archaeal ecological interaction network (AEIN) in TR exhibits higher net immigration rates, as well as resilience and energy-information efficiency. Archaeal community assembly in deep-sea wood fall is dominated by stochastic processes, which account for over 90% of assembly processes across all contact surfaces. The ecological functions of the archaeal community in TR are co-dominated by methane metabolism (65.7%) and nitrogen metabolism (34.3%), whereas those in SDCS and SWCS show pronounced enrichment in methane metabolism (97.6%) and nitrogen metabolism (100%), respectively. The archaeal diversity and interaction hub may serve as an indicator of the fastest-degrading zone in deep-sea wood fall. The TR may also provide diverse ecological niches that maintain this inherently unstable archaeal community. In addition, the prevalence of stochastic processes likely plays a crucial role in maintaining archaeal diversity. Furthermore, the archaeal community is critical to carbon, hydrogen, and nitrogen cycles within the deep-sea wood fall: methane metabolism is active in the archaeal community during the early and middle stages of wood-fall degradation, whereas nitrogen metabolism dominates the community's biogeochemical activities in the late stage. These findings provide new insights into the age and source of deep-sea wood falls in the SCS, and highlight the diversity, ecological functions, and biogeochemical processes of archaeal microbiota in deep-sea wood-fall ecosystems.

1. Introduction

The deep sea, which constitutes three-quarters of the total ocean area, is characterized by extreme conditions—including high pressure, low temperatures, low dissolved oxygen, and oligotrophy—that pose significant challenges to life. Contrary to its historical characterization as a "biological desert," the deep seafloor harbors hotspots of high biodiversity, including substantial microbial diversity, exemplified by deep-sea chemosynthetic ecosystems such as hydrothermal vents (Martin et al., 2008), cold seeps (Martin et al., 2008), whale falls (Li

This article is part of a special issue entitled: IPCA Ocean Interactions DSRII published in Deep-Sea Research Part II.

* Corresponding author. Guangxi Laboratory on the Study of Coral Reefs in the South China Sea; Coral Reef Research Center of China; School of Marine Sciences, Guangxi University, Nanning, China.
E-mail address: kefuyu@scsio.ac.cn (K. Yu).

https://doi.org/10.1016/j.dsr2.2026.105718
Received 22 October 2025; Received in revised form 19 October 2026; Accepted 2 November 2026
Available online 2 November 2026
0967-0645/© 2026 Elsevier Ltd. All rights are reserved, including those for text and data mining, AI training, and similar technologies.

et al., 2022), and wood falls (Bienhold et al., 2013). Unlike shallow-water ecosystems that rely on photoautotrophic nutrition, these chemosynthetic systems sustain a "dark food chain" that transports materials and energy throughout the deep sea (Stewart et al., 2005). Nearly all organic matter derived from land and surface ocean is degraded during its descent, leading to limited nutrient and energy availability in the deep sea (Stewart et al., 2005). Thus, large organic falls represent one of the key sources of nutrients and energy in this environment. When an organic fall settles on the oligotrophic seafloor, it can rapidly develop into a biodiversity hotspot, supporting a high-productivity ecosystem through the collaborative activities of benthic fauna and microorganisms recruited from the surrounding environment (Pop Ristova et al., 2017). Among these, wood falls represent a unique deep-sea ecosystems, characterized by their high lignocellulose content, broad geographical distribution, and function as wildlife corridors—providing habitats and nutritional resources for deep-sea organisms with limited dispersal capacity (Cunha et al., 2013). Most of the deep-sea floors is covered by soft sediments, with hard substrates being extremely scarce (Wolff, 1979). Thus, wood falls serve as critical habitats for benthic animals seeking hard substrates (Amon et al., 2017). Furthermore, wood-boring bivalves, through their wood-degrading activities, create cavities and grooves on wood surfaces, thereby increasing habitat complexity (Judge and Barry, 2016; Voight, 2015). These structures provide essential three-dimensional space and critical shelter for benthic colonizers such as tube worms, sponges, and hydroids (Harbour et al., 2021a,b).

Deep-sea wood falls (Distel et al., 2000; Kiel et al., 2009) provide unique habitats for specialized faunal-microbial symbioses (Dubilier et al., 2008). They also serve as "stepping stones" for specialist organisms among deep-sea chemotrophic ecosystems, as many endemic benthic organisms from these chemosynthetic habitats form interconnected populations linked via larval migration and dispersal (Pereira et al., 2020). For instance, Tandberg et al. (2013) documented the presence of *Pseudosetia griegi* and *Skenea profunda*—species typically associated with hydrothermal vents and cold seeps—in natural wood falls at 2830 m depth in the Norwegian Sea. Promoting biological evolution represents one of the most pivotal ecological functions of deep-sea wood falls. As a vital, rare, and hard-to-access resource in the deep sea, wood falls create selective pressures that drive the evolution of deep-sea species and enhance the efficiency of wood resource utilization. For example, Distel et al. (2002) identified a novel symbiotic bacterium, *Teredinibacter turnerae*, in the gill tissue of shipworms, which is characterized by its unique dual capacity to digest cellulose and fix nitrogen. This bacterium forms a specialized symbiosis with shipworms: it secretes cellulases to degrade wood debris and fixes atmospheric nitrogen to meet the host's nutritional needs during colonization of wood falls (Waterbury et al., 1983). Collectively, deep-sea wood fall ecosystems make substantial contributions to biodiversity, species evolution, and biogeochemical cycling in the global deep ocean (Distel et al., 2000; Kalenitchenko et al., 2015; Pereira et al., 2022).

Chemosynthetic microorganisms are foundational components of deep-sea chemosynthetic ecosystems. To survive under extreme environmental conditions, these microorganisms have evolved unique metabolic pathways and exceptional redox capabilities, thereby playing a pivotal role in global marine biogeochemical cycles (Jørgensen and Boetius, 2007). Accordingly, deep-sea wood-fall ecosystems not only serve as biodiversity hotspots in the oligotrophic abyss but also function as natural laboratories for investigating microbial adaptation to extreme environments and their contributions to elemental cycling. Studies have demonstrated that bacteria drive biogeochemical cycling in wood-fall ecosystems through diverse metabolic pathways involving sulfur, nitrogen, and methane, while fungi facilitate lignocellulose degradation by secreting a suite of lignocellulolytic enzymes (Bao et al., 2025). By contrast, despite the well-documented importance of archaeal communities in mediating critical steps of methane and nitrogen cycles in other chemosynthetic habitats (e.g., hydrothermal vents and cold seeps), their biogeochemical functions in wood-fall ecosystems remain largely undercharacterized (Fagervold et al., 2012; Moseley et al., 2022). Evidence indicates that organic inputs—including wood falls—can generate localized microbial diversity hotspots. For example, elevated archaeal α-diversity has been observed on pine and oak wood fragments near a shipwreck in the northern Gulf of Mexico (Moseley et al., 2022). However, the underlying mechanisms driving these diversity patterns, particularly for archaea, remain elusive. Furthermore, deciphering the community assembly mechanisms of archaea in wood falls is crucial for understanding the maintenance and enhancement of ecosystem functions and services (Jaillard et al., 2014; Wagg et al., 2014). Both deterministic processes (homogeneous selection and heterogeneous selection) and stochastic processes (homogenizing dispersal, dispersal limitation, and drift) are known to shape microbial communities in deep-sea wood fall ecosystems (Bao et al., 2025). While preliminary descriptions of archaeal community composition in these ecosystems exist (Fagervold et al., 2012; Kalenitchenko et al., 2015; Palacios et al., 2009), the mechanisms governing archaeal community assembly remain poorly understood. Specifically, the relative contributions of deterministic versus stochastic processes to shaping wood-fall archaeal communities are unclear. Collectively, the dispersal patterns and driving factors of microorganisms in deep-sea wood fall ecosystems remain largely unresolved, impeding our understanding of the formation and distribution of microbial α-diversity hotspots. Moreover, the archaeal community structure, ecological interaction networks, and functional potential across distinct wood interfaces—such as the seawater contact surface and sediment contact surface—are virtually uncharacterized. This spatial heterogeneity is ecologically significant, as distinct physicochemical gradients within each niche likely support specialized archaeal assemblages with unique functional roles. Therefore, a systematic investigation of archaeal communities across different wood interfaces—aimed at identifying diversity hotspots, elucidating community assembly mechanisms, and uncovering their driving biogeochemical processes—is essential for comprehensively understanding their ecological roles in wood-fall ecosystems.

This study was conducted on a deep-sea wood fall collected by the human-occupied vehicle (HOV) "*Shenhai Yongshi*" (Dive SY420, December 2021) at the Zhongnan Seamount in the South China Sea (SCS; Fig. 1). We employed AMS ^{14}C dating, micromorphological analysis, and biogeographic information integration to identify the species and origin of the wood fall. Additionally, using 16S rRNA gene amplicon sequencing, we analyzed the diversity, community composition, community structure, and potential biogeochemical functions of the archaeal community associated with the deep-sea wood fall. Simultaneously, we integrated molecular ecological network analysis to explore the co-occurrence patterns and topological features within the archaeal microbiota. Our results are expected to provide novel insights into the dynamics and interactions of archaeal microbiota in deep-sea wood fall, thereby contributing to a more comprehensive understanding of the driving mechanisms underlying community assembly and the biogeochemical processes mediated by prokaryotes in deep-sea wood-fall ecosystems.

2. Materials and methods

2.1. Sample collection, wood identification and AMS ^{14}C dating

In December 2021, the research vessel (R/V) "*Tansuo 2*" conducted "Cruise TS2-10-2" in the intermediate regions of the SCS, during which the Zhongnan Seamount was investigated. On December 23, 2021, during Dive SY420 operated by the HOV "*Shenhai Yongshi*" (Deep-Sea Warrior), a large natural wood fall (length: 125 cm, width: 38 cm, height: 14 cm; 115°30′6.96″ E, 14°01′9.95″ N) was discovered at a depth of 2321.6 m on the northern slope of the Zhongnan Seamount in the SCS (Fig. 1a and b). An entire deep-sea wood fall was collected, and 3-6 cm^3 wood fragments from the transition region (TR), sediment contact

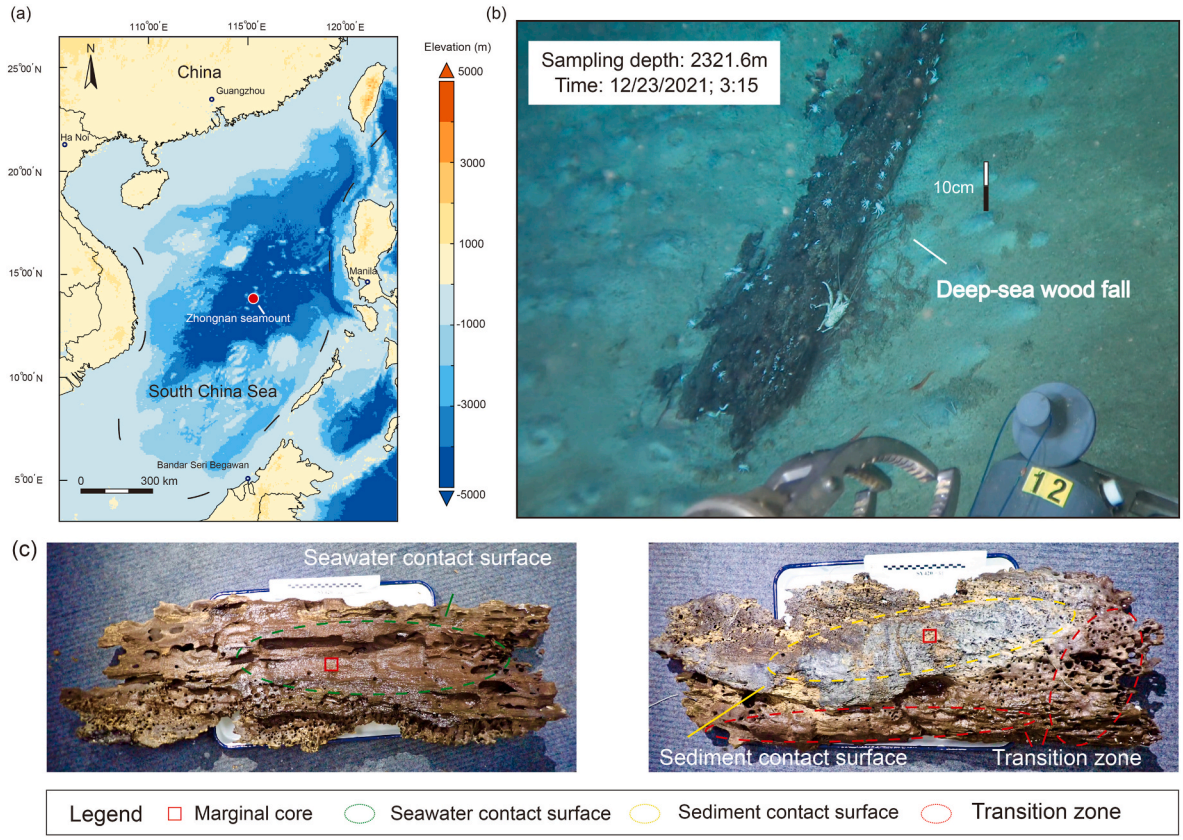


Fig. 1. Sampling location and contact surfaces of the deep-sea wood fall in the Zhongnan Seamount, South China Sea (SCS). (a) Sampling location of the deep-sea wood fall on the northern slope of the Zhongnan Seamount, SCS. (b) *In-situ* image of the deep-sea wood fall captured by the human-occupied vehicle HOV "*Shenhai yongshi*"; (c) Marginal core and contact surfaces of the deep-sea wood fall. These images were revised from Bao et al. (2025).

surface (SDCS), and seawater contact surface (SWCS) were transferred to 50 mL cryotubes and stored in liquid nitrogen for subsequent DNA extraction. The details of sample collection, grouping, and preservation followed the procedures described in previous study (Bao et al., 2025). While the present study focuses on the archaeal community, the bacterial and fungal data obtained from the same wood chip samples were analyzed separately in that earlier work (Bao et al., 2025). For wood species identification, 2-3 cm^2 fragments of the deep-sea wood fall were collected using a woodworking chisel. These fragments were softened by immersion in an ethyl alcohol:glycerin solution (1:1, v/v). The wood micromorphology was observed via light microscopy following the method described by Gregory and Jensen (2006): after softening, thin transverse, radial, and tangential sections (15-25 μm) were cut from each contact surface specimen using a LEICA CM3050S freezing microtome (Gregory and Jensen, 2006). Sections were stained with 1% (w/v) safranin in ethanol to enhance wood micromorphological features (Bao et al., 2025; Matthiesen et al., 2014). For AMS ^{14}C dating, 200 mg of the wood fall's marginal core was collected using a CO300 triple growth cone (Haglof, Sweden). Radiocarbon analysis was conducted at the Beta Analytic Testing Laboratory (Miami, USA). After bulk combustion, the acid-base-acid method was applied to clean the wood samples (Olsson, 1980). Wood ^{14}C ages were calibrated to calendar ages using the high-probability density (HPD) range method and the IntCal13 and NHZ3 datasets (Bronk Ramsey, 2009; Hua et al., 2013; Reimer et al., 2013).

2.2. DNA extraction, PCR amplification and next-generation sequencing

Total microbial DNA was extracted from wood fragments of the TR, SDCS, and SWCS using the FastDNA Spin Kit for Soil (MP Biomedicals, France). The concentration and purity of the extracted microbial DNA were determined using a NanoDrop 2000 ultraviolet spectrophotometer (Thermo Fisher Scientific, MA, USA). Only high-quality DNA samples—meeting the criteria of $1.8 < A260/A280 < 2.0$ and $A260/A230 > 2.0$—were selected as templates for PCR amplification. The V4-V5 hypervariable region of the archaeal 16S rRNA gene was amplified using primers 524F10extF (5′-TGYCAGCCGCCGCGGTAA-3′) and Arch958RmodR (5′-YCCGGCGTTGAVTCCAATT-3′) (Liu et al., 2016). This primer set provides broad phylogenetic coverage of major archaeal lineages, including Euryarchaeota, Thaumarchaeota, and Bathyarchaeota, while correcting the amplification bias against Thaumarchaeota typically associated with conventional archaeal primers. The amplicon length (~450 bp) is optimal for paired-end sequencing on the Illumina platform. Moreover, this primer combination has been successfully validated in complex environments such as mangrove sediments (Pires et al., 2012), ensuring robust and comparable community analysis in this study. PCR was performed with ~10 ng of DNA, 1.6 μL (5 μm) primer, 0.4 μL TransStart Fastplu DNA Polymerase, 0.2 μL BSA, 4 μL 5 × FastPfu Buffer, 2 μL of 2.5 mM dNTPs, and ddH_2O to a total volume of 20 μL. GeneAmp® 9700 thermocycle controller was used to carry out PCR amplification with the following programme: 3 min at 95 °C, followed by 29 cycles of 95 °C for 30 s, 53 °C for 30 s, 72 °C for 45 s, and final extension at 72 °C for 10 min. Purifying of PCR products was conducted using Qiagen Agarose Gel DNA Purification kit (Qiagen, Hilden, Germany). The amplicon sequencing of archaeal 16S rRNA V4-V5 region was performed on an Illumina Miseq platform using the 2×300 bp mode according to standard protocols at Majorbio (Shanhai, China). The raw 16S reads were deposited into the NCBI Sequence Read Archive database (Accession Number: PRJNA1221359).

2.3. Data processing and bioinformatic analysis

Archaeal sequence data processing was performed using the Quantitative Insights Into Microbial Ecology 2 (QIIME 2) framework (version 2018.8) (Bolyen et al., 2019). Briefly, Samples were stratified by sequencing lane for error rate learning and amplicon sequence variant (ASV) inference with DADA2 (Callahan et al., 2016). Forward and reverse ASVs were subsequently merged, and chimeric sequences were filtered out via the package's native chimera-detection functions. ASVs accounting for fewer than six total inserts were flagged as spurious and excluded from the dataset. Taxonomic classification of archaeal 16S rRNA gene ASVs was conducted within the QIIME 2 platform using a naive Bayes classifier. This classifier aligned ASVs against the Silva v138 16S rRNA gene database (archaea-specific subset), with a bootstrap confidence threshold of 0.7 set for taxonomic assignment (Bokulich et al., 2018). All samples were normalized to the lowest number of sequences (3,019). Additionally, sequences derived from mitochondria, chloroplasts, and non-archaeal sources, were removed from the dataset to ensure data purity. Downstream analyses—including the calculation of ecological indices, construction of microbial ecological interaction networks, and analysis of topological features—were performed using high-confidence archaeal ASVs.

2.4. Ecological indices analyses and potential function prediction

The Observed ASVs and Shannon diversity index were used to assess the α-diversity of archaeal communities across different contact surfaces of the deep-sea wood fall. These indices were calculated using the high-confidence ASV dataset with the Vegan package in R (Oksanen et al., 2015). Significant differences in archaeal α-diversity among contact surfaces were analyzed via the Kruskal-Wallis test using GraphPad Prism 8 (version 8.3.0); the Tukey-Kramer test was employed for post-hoc multiple comparisons following significant Kruskal-Wallis results. Archaeal community composition at the phylum and family levels across contact surfaces was visualized using the ggplot2 package in R. Permutational multivariate analysis of variance (PERMANOVA) was used to determine the significance of differences in archaeal community structure among the transition region (TR), sediment contact surface (SDCS), and seawater contact surface (SWCS). This analysis was based on 9999 permutations of the Bray-Curtis dissimilarity matrix. Principal Coordinates Analysis (PCoA) was performed to visualize PERMANOVA results, using the Bray-Curtis distance metric with the Vegan package in R (Oksanen et al., 2015). To characterize archaeal community assembly processes, the β-nearest taxon index (βNTI) and Bray-Curtis-based Raup-Crick matrix (RCbray) were calculated. A value of $|\beta NTI| < 2$ indicated that community assembly was primarily driven by stochastic processes. For pairwise community comparisons that did not deviate from the null model, RCbray values were used to quantify the contribution of homogenizing dispersal (RCbray < -0.95) and dispersal limitation (RCbray > 0.95). When $|RCbray| < 0.95$, community assembly was attributed to undominated processes—reflecting weak dispersal, weak selection, diversification, and drift. In contrast, $|\beta NTI| > 2$ indicated deterministic processes: $\beta NTI > 2$ represented heterogeneous selection, while $\beta NTI < -2$ represented homogeneous selection (Allen et al., 2020; Zhou and Ning, 2017). SourceTracker (version 0.9.8)—a Bayesian microbial source-tracking tool—was used to estimate the sources of archaeal communities across wood fall contact surfaces (Knights et al., 2011). We performed three independent SourceTracker analyses. In each analysis, samples from one contact surface were iteratively designated as the "sink" (target community), while samples from the remaining two contact surfaces were designated as candidate "sources" (potential contributing communities). Microbial taxa not originating from any of the designated potential sources were classified as "unknown." This analysis was used to evaluate microbial transmission and contribution patterns of archaeal communities among contact surfaces. The average variation degree (AVD) was used to assess archaeal community stability, calculated based on the degree of deviation from the mean of normally distributed ASV relative abundances across contact surfaces. Higher AVD values indicated lower community stability. AVD was calculated following the method described by Xun et al. (2021), and statistical results were visualized using the ggplot2 package in R. Additionally, Functional Annotation of Prokaryotic Taxa (FAPROTAX) was employed to predict the potential ecological functions of archaeal communities across wood fall contact surfaces (Louca et al., 2016).

2.5. Molecular ecological network inference and topological features analysis

To explore potential interactive relationships and modular structures within the archaeal microbiota of deep-sea wood fall, an archaeal ecological interaction network (AEIN) was constructed across different contact surfaces using the CoNet plugin in Cytoscape 3.9.1 (Faust and Raes, 2012; Shannon et al., 2003). Briefly, the ecological interaction network was inferred with archaeal ASVs as nodes, following two screening criteria: archaeal ASVs were required to be present in at least two samples and have more than 25 reads. Pairwise correlations of archaeal ASVs across the deep-sea wood fall and its distinct contact surfaces were estimated using five metrics: two dissimilarity measures (Bray-Curtis and Kullback-Leibler dissimilarities), two correlation measures (Pearson and Spearman correlations), and one similarity measure (mutual information). Initially, 1000 positive and 1000 negative links were retrieved as initial thresholds for these five metrics. To mitigate combinatorial bias, 1000 normalized permutations and 1000 bootstrap scores were generated. Brown's method was employed to merge and calculate measure-specific p-values (Brown, 1975). The Benjamini-Hochberg procedure was used to correct for multiple comparisons, with edges retained only if their merged p-values were below 0.05 (Benjamini and Hochberg, 1995). Subsequently, visualization of the AEIN was performed using Gephi 0.9.7 and Cytoscape 3.9.1.

To characterize the topological features of AEIN in deep-sea wood fall and distinct contact surfaces, the number of nodes, number of edges, network diameter, average degree, clustering coefficient, average path length, complexity, betweenness centrality and modularity have been calculated using igraph package in R. In general, the network diameter defined as indicator of scale of AEIN (Yuan et al., 2021). The average number of interactions per node has been indicated by average degree, which suggest the intensity of archaeal interaction (Jiao et al., 2020; Ma et al., 2016). The clustering coefficient was defined as a measure of degree to which nodes in a network tend to cluster together, which closely associate stability and robustness of AEIN structure (Jiao et al., 2020; Yuan et al., 2021). The average path length was used to test the shortest network distance between archaeal taxa, which can be employed to assess the efficiency of information and energy transmission within the AEIN (Deng et al., 2012; Zhang et al., 2020). The number of nodes and edges was used to calculated to linkage density (links per node) of AEIN, which have been suggest to reflect the complexity of AEIN. In addition, the betweenness centrality has been suggested to indicated the resilience and connectivity of microbial community (Estrada-Peña et al., 2018; Lima et al., 2020), which calculates the shortest path through a AEIN and keeps record of how many times a node in a network is traversed (Freeman, 1977). The modularity was used to determine the niche differentiation and specialization of archaeal community among contact surfaces in deep-sea wood fall (Liu et al., 2022).

3. Results

3.1. Geochronological and morphological features of wood fall

After calibration against the IntCal13 and NHZ3 databases, the ^{14}C age of the marginal portion of the deep-sea wood fall core was

determined to range from −30 to −32 cal BP (Table 1). This indicates that the tree from which the wood sample originated ceased growing between 1979 and 1981. Thus, it can be inferred that the deep-sea wood fall formed after the 1970s (Fig. 1c). For wood identification, the sample displays indistinct growth rings and is diffuse-porous. In cross section, the vessels are circular to elliptical, occurring as single pores or occasionally in short radial multiples of 2-3 (Fig. 2a). Axial parenchyma in cross section is scattered or forms marginal vasicentric to vasicentric bands (Fig. 2b). The wood fibers are thin-walled with bordered pits and include fiber-tracheids. The rays are both uniseriate and multiseriate, classified as heterogeneous Type II (Fig. 2c). Comprehensive analysis of the morphological characteristics of the wood sections confirmed that the studied deep-sea wood fall is *Homalium hainanense* Gagnep. Notably, according to records from the Global Biodiversity Information Facility (GBIF), *H. hainanense* Gagnep. is distributed exclusively in China and Vietnam (Fig. 2d), with the highest number of recorded habitats (n = 11) in Hainan Province, northern SCS.

3.2. The diversity of archaea community

After quality control and filtering of the reads, 835,814 sequences were aligned against archaeal reference databases and clustered into ASVs following dataset subsampling. A total of 6 phyla, 5 classes, 5 orders, 5 families, and 50 ASVs were identified from the deep-sea wood fall. Observed ASVs analysis revealed a significant difference in archaeal community richness among the contact surfaces of the deep-sea wood fall (Kruskal-Wallis test, $p = 0.012 < 0.05$; Fig. 3a), with the richness in the TR being significantly higher than that in the SWCS. Additionally, archaeal communities exhibited significant differences in Shannon diversity index among the wood fall's contact surfaces (Kruskal-Wallis test, $p = 0.014 < 0.05$; Fig. 3b). The diversity of archaeal community in TR was also significantly higher than that in SWCS, which was consistent with the results of the richness analysis. These results suggest that the center of archaeal community diversity is located in the TR of the deep-sea wood fall.

3.3. The community composition and potential source of archaea

At the phylum level, six archaeal phyla were identified in the deep-sea wood fall community: Euryarchaeota (73.75%), Nitrososphaerota (19.58%), Crenarchaeota (1.88%), Candidatus Thermoplasmatota (1.46%), Pacearchaeota (0.14%), and Thermoproteota (0.21%) (Fig. 4a). Euryarchaeota was ubiquitous and dominant across all contact surfaces, with a relative abundance ranging from 40.83% to 90.42%. In contrast, Nitrososphaerota exhibited high relative abundance in the SDCS (55.00%) and SWCS (22.50%) but was rare in the TR (0.42%). Crenarchaeota was present across all wood fall contact surfaces (TR: 1.67%; SDCS: 0.83%; SWCS: 3.33%) but with a relative abundance of less than 5%. Candidatus Thermoplasmatota, Pacearchaeota, and Thermoproteota had restricted distributions within the wood fall (Fig. 4a): Candidatus Thermoplasmatota was detected in TR (2.08%) and SDCS (1.67%) but not in SWCS; Pacearchaeota was exclusive to TR (0.42%); and Thermoproteota was only found in SWCS (0.83%). At the family level, five annotated families were identified, with Halobacteriaceae (24.31%) and Methanobacteriaceae (39.03%) dominating the archaeal community. Notably, Methanomassiliicoccaceae was limited to TR (2.08%) and SDCS (1.67%), while Methanosarcinaceae occurred solely in SDCS (2.5%; Fig. 4b), suggesting a distinct distribution pattern of these methanogenic archaea within the wood fall. Nitrososphaeraceae was detected across all contact surfaces, with a relative abundance ranging from 0.42% to 1.67%. Additionally, five archaeal taxa could only be annotated at the phylum level, with their relative abundances ranging from 0.14% to 25.00% (Fig. 4b).

The PCoA and PERMANOVA analysis results showed that there were significant differences of archaea community structure among contact surfaces in deep-sea wood fall (PERMANOVA, $f = 2.006$, $R^2 = 0.2358$, $p = 0.023 < 0.05$; Fig. 4c). SourceTracker was employed to trace the sources of archaeal microbiota across distinct contact surfaces. The results showed that the majority of archaeal sources remained unknown for all contact surfaces (TR: 87.8 ± 4.3%; SDCS: 89.1 ± 18.7%; SWCS: 90.8 ± 11.3%; Fig. 4d). Notably, the TR archaeal community contributed 3.4 ± 2.7% to the other contact surfaces (SDCS: 4.0 ± 1.6%; SWCS: 2.8 ± 3.4%; Fig. 4d). Conversely, TR served as a sink for archaeal microbiota from SDCS and SWCS, with source contributions of 7.2 ± 8.2% and 5.0 ± 9.2%, respectively—indicating that sink contribution exceeded source contribution for the TR archaeal community. Additionally, SDCS contributed 6.4 ± 12.8% of archaeal microbiota to SWCS, while SDCS also received 6.9 ± 0.7% of its archaeal community from SWCS (Fig. 4d).

3.4. The archaea community assembly and stability

The assembly of archaeal communities in the deep-sea wood fall was primarily controlled by stochastic processes, with the percentages of pairs in the TR, SDCS, and SWCS being 93.8%, 91.7%, and 96.7%, respectively (Fig. 5a and b). Across distinct contact surfaces, the assembly of archaeal communities was mainly driven by drift (TR: 86.5%; SDCS: 83.3%; SWCS: 86.7%) and homogenizing dispersal (TR: 5.2%; SDCS: 8.3%; SWCS: 10.0%; Fig. 5c). However, archaeal community turnover was also shaped by heterogeneous selection—a deterministic process—accounting for 3.1%, 8.3%, and 3.3% of assembly in TR, SDCS, and SWCS, respectively (Fig. 5c). Notably, the archaeal community in TR exhibited the most diverse assembly processes: its turnover was influenced not only by heterogeneous selection (3.1%) and homogeneous selection (3.1%) but also regulated by dispersal limitation (2.1%; Fig. 5c). To assess the stability of archaeal communities within the wood fall, the AVD among contact surfaces was calculated. The results revealed significant differences in the AVD values of archaeal communities across the wood fall's contact surfaces (Kruskal-Wallis test, $p = 0.004 < 0.05$; Fig. 5d), with the degree of variation in TR and SDCS being significantly higher than that in SWCS. This suggests that the archaeal community in SWCS possesses stronger stability than those in TR and SDCS.

3.5. The ecological interaction network and potential function of archaea community

CoNet analysis revealed diverse potential interactive relationships and modular structures within the archaeal microbiota of the deep-sea wood fall (Fig. 6a). The topological features of the AEIN exhibited substantial variations across different contact surfaces of the deep-sea wood fall (Fig. 6b). The number of nodes and links in the AEIN ranged from 4 to 32 and 2 to 48, respectively. Specifically, the AEIN in the TR had more nodes (32), edges (48), and a larger diameter (4) compared to the SDCS (nodes: 13, edges: 16, diameter: 1) and SWCS (nodes: 4, edges: 2, diameter: 1). This indicates that the AEIN in TR was larger in scale than those in the other two contact surfaces. Additionally, the average degree of the AEIN ranged from 1.00 to 3.00, confirming that the interaction strength of the archaeal microbiota was higher in TR (3.00) than in SDCS (2.46) and SWCS (1.00). Notably, the variation pattern of

Table 1
Radiocarbon ages of marginal core of deep-sea wood fall in the Zhongnan seamount of the South China Sea.

Sample Type	Dating method	^{14}C calibrated age (cal·BP)	Calibration of ^{14}C age to calendar years
marginal core of deep-sea wood fall	Accelerator Mass Spectrometry (cAMS) radiocarbon-14 dating method	−30 ~ −32 cal BP[a]	1979-1981 cal AD

[a] ^{14}C age relative to 1950, with an uncertainty of 1σ.

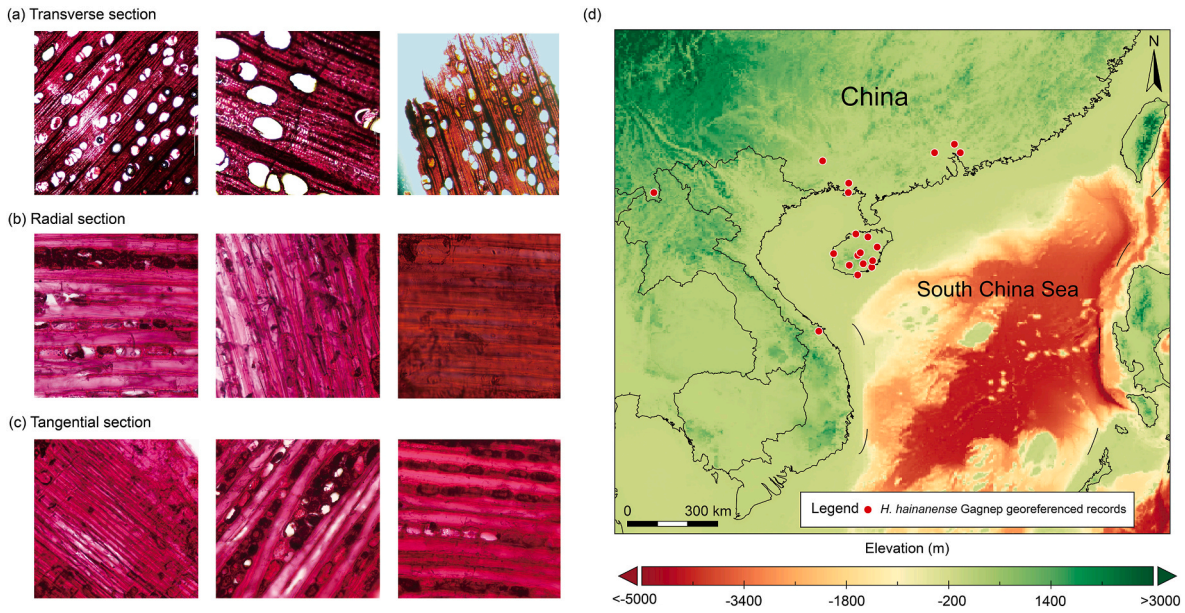


Fig. 2. Micromorphology of the deep-sea wood fall and biogeographic distribution of *Homalium hainanense* Gagnep. (a) Transverse section of the wood sample; (b) Radial section of the wood sample; (c) Tangential section of the wood sample; (d) Biogeographic distribution of *H. hainanense* Gagnep. based on data from the Global Biodiversity Information Facility (GBIF; https://www.gbif.org/).

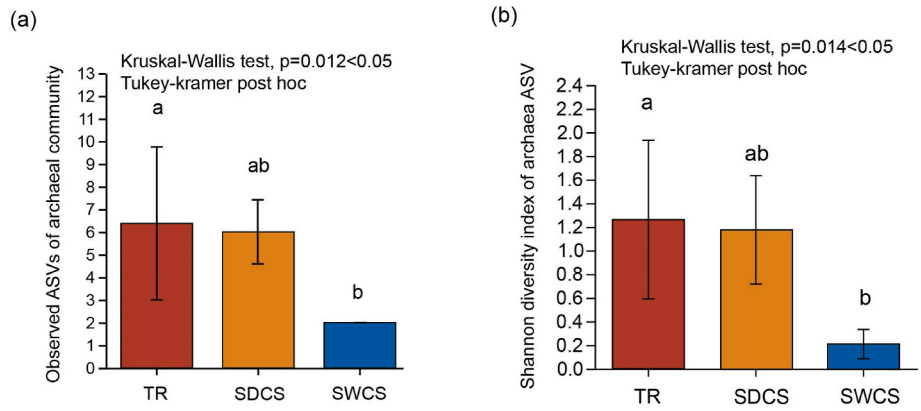


Fig. 3. α-Diversity of archaeal communities among contact surfaces of the deep-sea wood fall. (a-b) Significant differences in the Observed ASVs and Shannon diversity index of archaeal communities among wood fall contact surfaces.

the clustering coefficient differed from that of other topological indices: the archaeal microbiota in SDCS exhibited the highest clustering coefficient (0.988; Fig. 6b), and the average fraction of clustered pairs was higher in TR (0.924) and SDCS than in SWCS (0.000). These results suggest that the structural robustness of the AEIN was stronger in SDCS and TR than in SWCS. The average path length of the AEIN was lower in SDCS (1.000) and SWCS (1.000) than in TR (1.930; Fig. 6b), indicating higher energy and information transfer efficiency of the AEIN in TR compared to SDCS and SWCS. Furthermore, the AEIN in TR exhibited higher complexity (1.500) and betweenness centrality (2.906) than those in SDCS (complexity: 1.231, betweenness centrality: 0) and SWCS (complexity: 0.5, betweenness centrality: 0). The modularity values of the AEIN were 0.737 (TR), 0.680 (SDCS), and 0.500 (SWCS), respectively (Fig. 6b). Collectively, these findings demonstrate that the AEIN in TR had stronger stability, higher complexity, and greater resilience than those in SDCS and SWCS within the deep-sea wood fall. Moreover, the clustering coefficient, average path length, betweenness centrality, and modularity of the total AEIN in TR were all higher than those of the entire deep-sea wood fall microecosystem.

FAPROTAX was employed to predict the ecological functions of archaeal communities across different contact surfaces of the deep-sea wood fall. Sequences of the archaeal microbiota were assigned to three primary functional categories: methane metabolism, nitrogen metabolism, and chemoheterotrophy, with the contributions of these potential functions varying significantly among contact surfaces (Fig. 7). The ecological functions of the archaeal community in the transition region (TR) were co-dominated by methane metabolism (65.7%) and nitrogen metabolism (34.3%). Specifically, functional processes including methanogenesis (21.9%), hydrogenotrophic methanogenesis (21.9%), and dark hydrogen oxidation (21.9%) were identified in this region. Additionally, the archaeal microbiota in TR fulfilled an important ecological role in anaerobic ammonia oxidation (17.2%) and nitrification (17.1%; Fig. 7a). In contrast, sequences of the archaeal community in the sediment contact surface (SDCS) were predominantly predicted to be involved in methane metabolism (97.6%), with a minor contribution from chemoheterotrophy (2.4%). Four functional traits were identified in SDCS: methanogenesis (33.3%), hydrogenotrophic methanogenesis (31.0%), methanogenesis by disproportionation of methyl groups (2.3%), and dark hydrogen oxidation (31.0%), whereas chemoheterotrophy accounted for only 2.4% of the community's

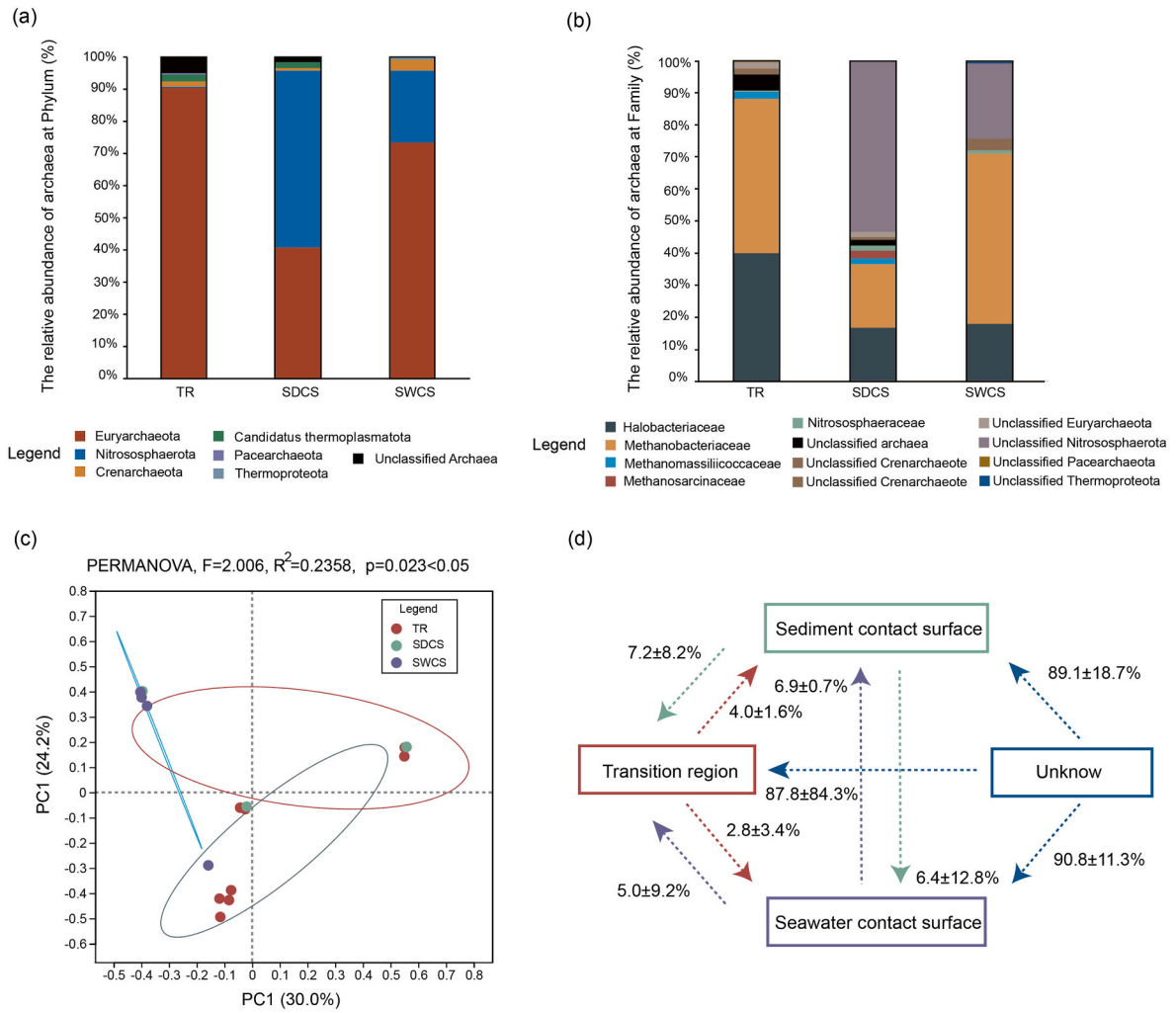


Fig. 4. Composition and structure of archaeal communities among contact surfaces of the deep-sea wood fall. (a-b) Relative abundance of archaea at the phylum and family levels. (c) Principal Coordinates Analysis (PCoA) of Bray-Curtis distances for archaeal ASV compositions across the three contact surfaces. (d) Source resolution of archaeal communities among the three contact surfaces.

functional potential (Fig. 7b). Notably, almost all sequences of the archaeal community in the seawater contact surface (SWCS) were assigned to anaerobic ammonia oxidation (50.0%) and nitrification (50.0%), indicating that SWCS serves as the functional core zone for nitrogen metabolism (100.0%) of the archaeal microbiota within the deep-sea wood fall (Fig. 7c).

4. Discussion

4.1. The wooden vessels is considered to be a potential cause of deep-sea wood fall

The results of morphological analysis revealed that the deep-sea wood fall was identified as *H. hainanense* Gagnep. (Fig. 2a). The natural distribution of *H. hainanense* Gagnep. has been reported to include China (with its primary range in Hainan Province) and Vietnam (Fig. 2d). Notably, *H. hainanense* Gagnep. serves as a core material in wooden vessel construction in the SCS (Chen et al., 1992; Yao, 1988), owing to its high density (0.675-0.819 g/cm^3), flexural strength (1142 kgf/cm^2), hardness (transverse section: 1.033 kgf/cm^2; radial section: 840 kgf/cm^2; tangential section: 930 kgf/cm^2), and corrosion resistance (Chen et al., 1992; Yao, 1988). Consequently, *H. hainanense* Gagnep. was commonly used in constructing keels, bottom planks, rudder boards, and hulls of wooden fishing vessels in Hainan Province, China (Chen et al., 1992). Prior to 1986, China's Hainan Province could only produce wooden fishing vessels, primarily including wooden sailing fishing boats, motor-sailing fishing boats, and wooden fishing trawlers (Li, 2009). Notably, ^{14}C dating of the marginal core indicates that the tree from which the wood fall originated ceased growing between 1979 and 1981. This suggests the deep-sea wood fall formed after the 1970s (Fig. 1c). The discovery site of the wood fall-the Zhongnan Seamount-overlaps with the traditional fishing grounds of Hainan fishermen, specifically the "Xisha-Zhongsha Fishing Ground" and "Nansha Fishing Ground" (Li, 2009). These findings suggest a close link between the occurrence of deep-sea wood fall and wooden vessels from the post-1970s period.

4.2. High archaeal diversity and ecological interaction centrality suggest accelerated TR degradation in deep-sea wood fall

In this study, the archaeal community in the TR of the deep-sea wood fall exhibited higher α-diversity (based on the Observed ASVs and Shannon diversity index) than those in other contact surfaces. Additionally, AEIN analyses revealed that the topological features of the AEIN in TR were generally higher than those in the SDCS and SWCS. This indicates that the AEIN of the TR archaeal community has a larger scale, greater stability and resilience, and higher energy and information transfer efficiency. These results indicated that the archaeal community

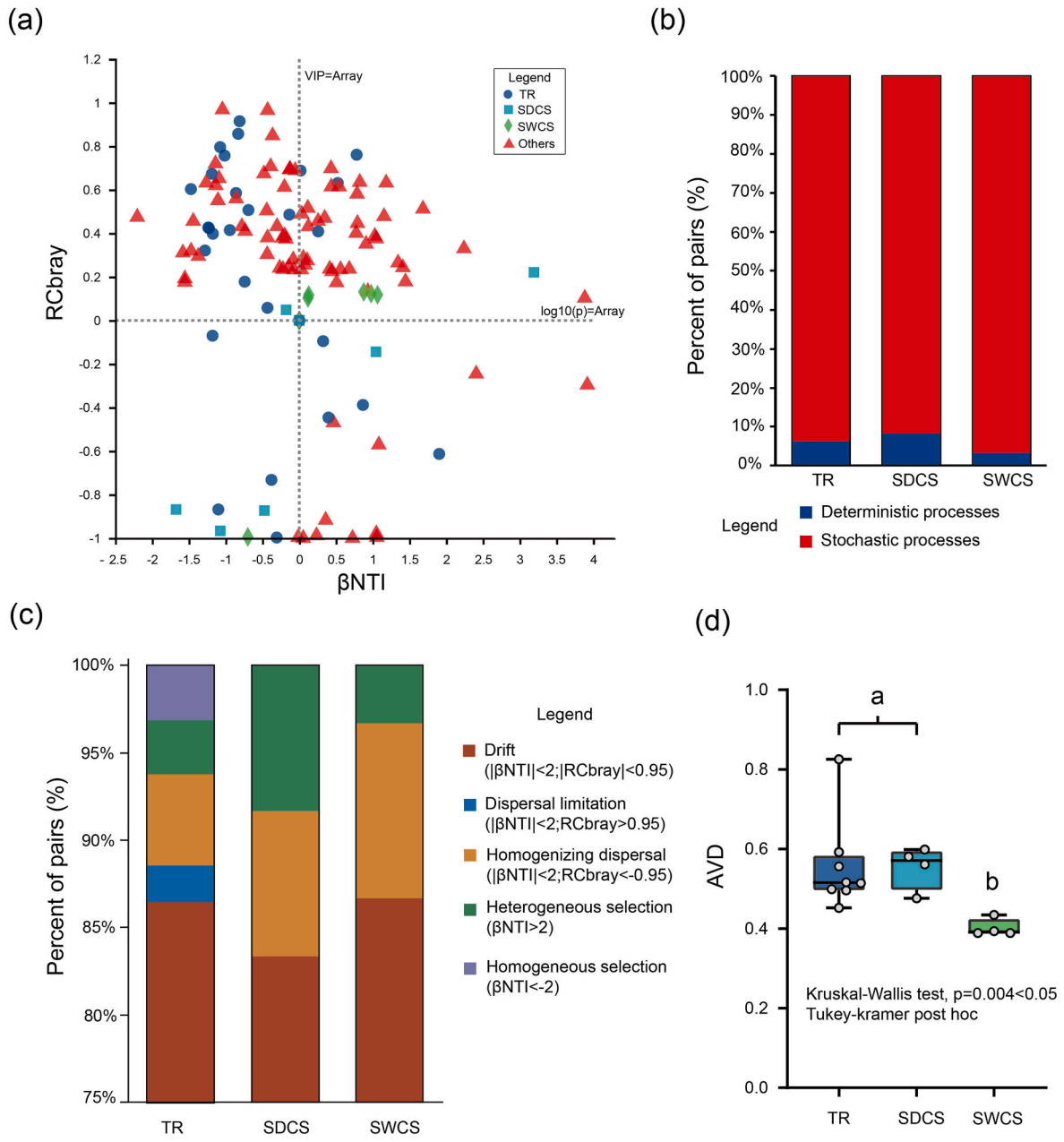


Fig. 5. Assembly processes and stability of archaeal communities among distinct contact surfaces of the deep-sea wood fall. (a) Relationship between the β-nearest taxon index (βNTI) and Bray-Curtis-based Raup-Crick matrix (RCbray) for the wood fall archaeal community; (b) Relative influence of archaeal community assembly processes, characterized by the percentage of contact surfaces governed by deterministic vs. stochastic processes; (c) Contributions of drift, dispersal limitation, homogenizing dispersal, heterogeneous selection, and homogeneous selection to archaeal community assembly across contact surfaces; (d) Average variation degree (AVD) of archaeal communities among wood fall contact surfaces. TR: transition region; SDCS: sediment contact surface; SWCS: seawater contact surface.

forms a diversity and ecological interaction center in the TR of the deep-sea wood fall, and TR has more rapidly degradation rate. Previously studies found that archaea widely distributed in the sediments in deep sea, but it was only identified in the visibly decayed deep sea wood fall and surrounding sediments (Fagervold et al., 2012; Kalenitchenko et al., 2015; Palacios et al., 2009). For example, an archaeal community analysis of ten types of sunken wood submerged for over a year in the Pacific Ocean and the Mediterranean Sea revealed that archaeal populations were only detected in wood samples showing substantial signs of decay, and that community compositions from samples with longer immersion times were highly similar despite their different oceanic origins (Palacios et al., 2009). It is noteworthy that the alpha diversity of microbial communities in short-term deep-sea wood falls was lower than that in wood falls subjected to long-term immersion (Fagervold et al., 2012). Thus, the diversity and interaction network hub of the archaeal community overlaps with the zone of maximum decomposition in deep sea wood fall. In addition, Bao et al. (2025) found that the total carbon and total nitrogen contents in TR were significantly lower than those in SDCS and SWCS, and that the hemicellulose and lignin contents were at low levels (Bao et al., 2025). A decrease in lipid concentration was also identified in the 360-day time-series wood-fall experiment using oak and pine wood (Kalenitchenko et al., 2015). These studies indicated that the TR zone is characterized by greater nutrient consumption and more rapid degradation. Consequently, the biodiversity and interaction hub of the archaeal community has the potential to serve as an indicator of the fastest-degrading zone in deep-sea wood fall, and the TR zone may represent the most rapidly decomposing interface among all micro-habitats within this wood fall. Notably, source tracking analysis showed

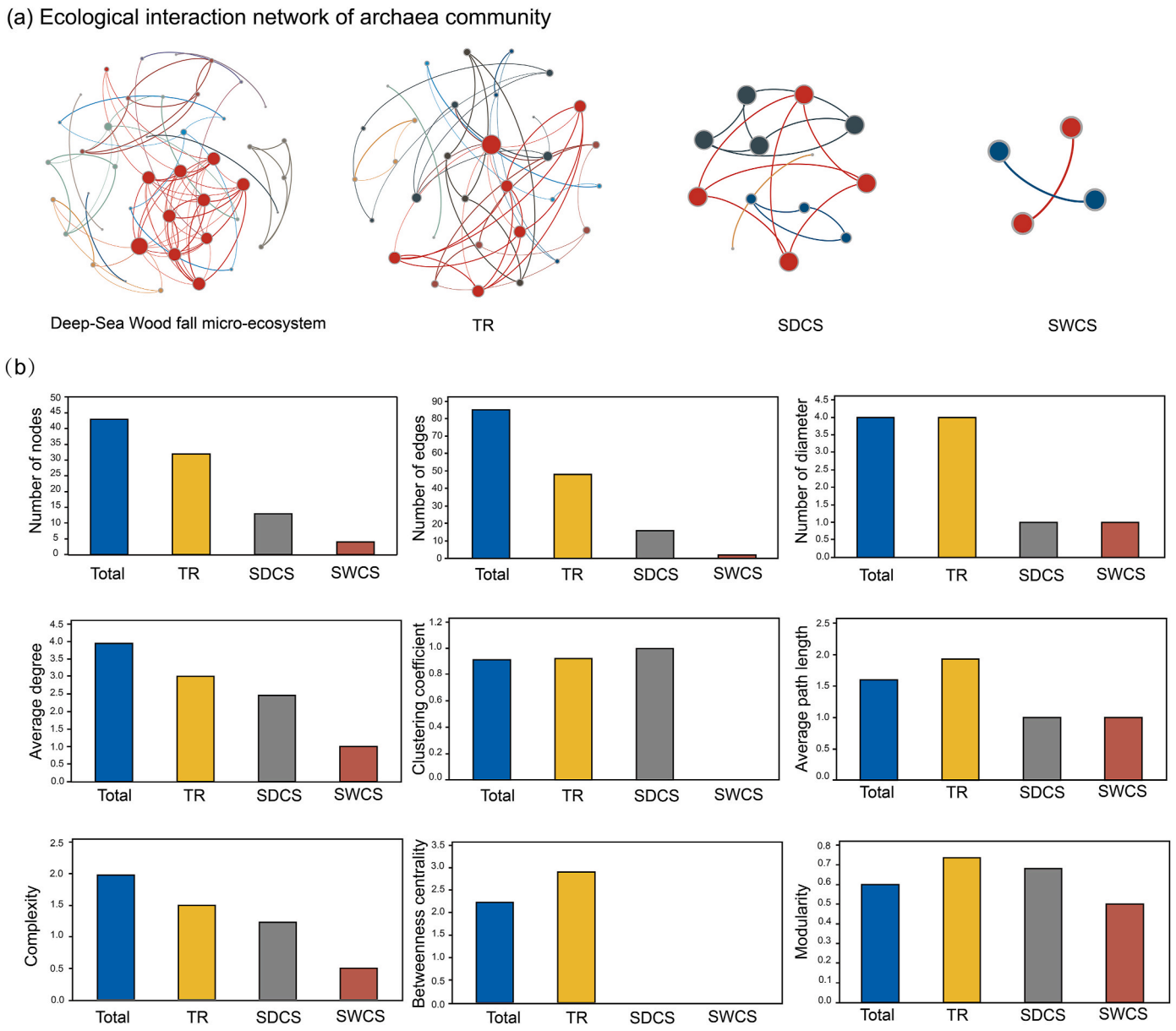


Fig. 6. Ecological interaction networks and topological properties of archaeal communities in the deep-sea wood fall. (a) Visualization of constructed archaeal co-occurrence networks for the entire wood fall and individual contact surfaces; all modules are represented by distinct colors. (b) Topological features of archaeal ecological interaction network (AEIN) for the entire wood fall and individual contact surfaces. (For interpretation of the references to color in this figure legend, the reader is referred to the Web version of this article.)

that the sink contribution of the TR archaeal community to SDCS and SWCS was 6.1 ± 8.7%—higher than its source contribution (3.4 ± 2.7%). Although the sources for a lot of archaeal taxa in TR remained unknown, this results also indicated that the archaeal community of TR has more taxa from the other contact surface, which has higher immigration rate of archaea than that of SDCS and SWCS. Therefore, the formation of diversity and ecological interaction center may closely associate with dispersal process.

Nevertheless, analysis of the average variance of pairwise distances (AVD) revealed that the TR archaeal community exhibited greater variation than that in SWCS (Fig. 5d), indicating that although the archaeal diversity and interaction hub was located in TR, its community structure remained relatively unstable (Xun et al., 2021). In contrast, ecological network analysis showed that the TR archaeal community possessed the highest modularity (Fig. 6), suggesting that TR provides the most diverse niches for these inherently unstable archaeal communities in deep-sea wood fall (Liu et al., 2022; Zhou et al., 2010). This niche diversity may play an important role in maintaining the archaeal diversity hub.

Collectively, the archaeal diversity and interaction hub has the potential to indicate the zone of fastest degradation in wood fall, and this zone is most likely the TR. The dispersal process may also be associated with the formation of this archaeal diversity and interaction center. Although the archaeal community structure within TR is not stable, this zone may provide diverse ecological niches that help sustain archaeal microbiota in deep-sea wood fall.

4.3. The community assembly processes closely associated with archaeal diversity maintenance and microhabitats complexity of deep-sea wood fall

Microbial community assembly is mainly described as being driven by two types of processes under different environmental conditions: stochastic processes (homogenizing dispersal, dispersal limitation, and drift) and deterministic processes (homogeneous selection and

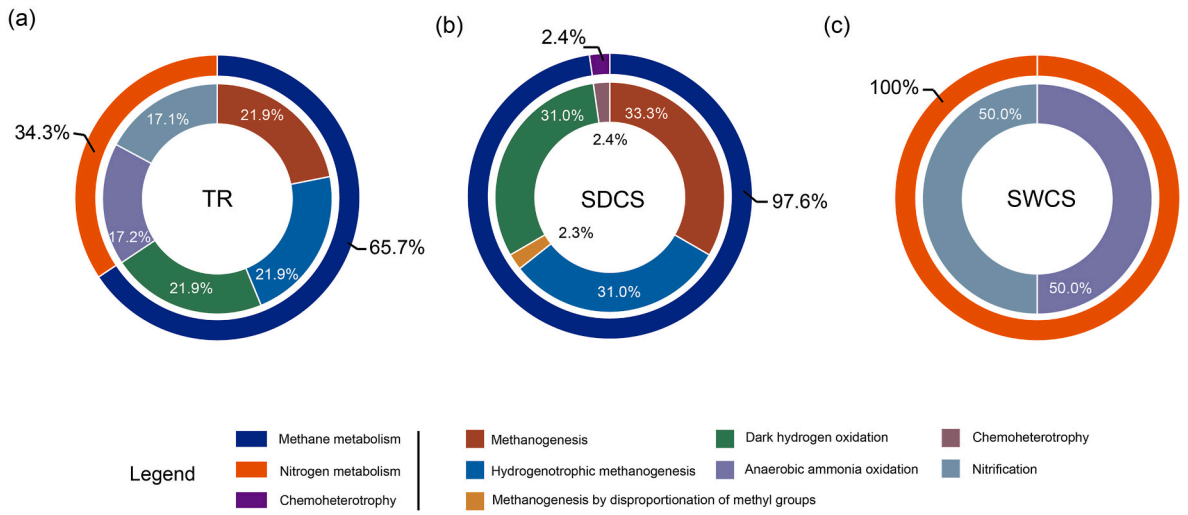


Fig. 7. Potential ecological functions of archaeal communities in the deep-sea wood fall. Ecological functions of archaeal microbiota predicted by FAPROTAX for (a) the transition region (TR), (b) sediment contact surface (SDCS), and (c) seawater contact surface (SWCS) of the wood fall, based on 16S rRNA gene data.

heterogeneous selection) (Nemergut et al., 2013; Wen et al., 2022; Zhou and Ning, 2017). In deep-sea wood falls, archaeal community assembly is primarily controlled by stochastic processes, which may be closely associated with abundant nutrient supply and high productivity. Notably, wood falls—rich in organic matter—are among the key nutritional and energy sources for the oligotrophic deep ocean (Bienhold et al., 2013). They can significantly enhance productivity by attracting chemoautotrophic microorganisms and benthic animals, thereby creating biodiversity hotspots in low-temperature, high-pressure deep-sea environments (Bertolaso et al., 2015; Pereira et al., 2022; Pop Ristova et al., 2017). Previous studies have shown that stochastic processes exert a greater influence on community assembly in more productive environments, particularly when other environmental factors do not impose dominant selection pressures (Chase, 2010). For instance, in the oligotrophic South Pacific, the contribution of stochastic processes was significantly higher in the deep chlorophyll maximum (DCM) layer than in surface waters (Allen et al., 2020). Furthermore, compared to deterministic processes, stochastic community assembly may play a more critical role in generating and underlying high biodiversity in productive habitats. Shifts in community assembly processes are one of the reasons for the formation of diverse ecological regimes across the planet (Chase, 2010). Thus, stochastic community assembly is likely crucial for maintaining archaeal diversity in deep-sea wood fall ecosystems.

In summary, archaeal community assembly in deep-sea wood fall is primarily driven by stochastic processes, which may play important roles in sustaining archaeal diversity within this microecosystem. The complex microhabitats of deep-sea wood fall further promote the diversification of archaeal community assembly processes.

4.4. Archaea microbiota play a driving role in the nitrogen and methane metabolism patterns in deep-sea wood fall

Analysis of the archaeal community revealed that methanogenic archaea exhibited high relative abundance in the deep-sea wood fall, with dominance by the families Methanobacteriaceae, Methanomassiliicoccaceae, and Methanosarcinaceae (Fig. 4). However, functional prediction results indicated that archaeal microbiota-driven methanogenesis occurred in the TR and SDCS, where these archaeal taxa were enriched with methylotrophic methanogens (Fig. 7a and b) (Fagervold et al., 2012). In contrast, the archaeal community in the seawater contact surface (SWCS) lacked potential methanogenic genes (Fig. 7c). These results suggest that archaeal community-driven methanogenesis and dark hydrogen oxidation played critical roles in the carbon-hydrogen cycle of the deep-sea wood fall. Archaeal-associated methane metabolism likely occurred during the early to middle stages of wood degradation, coinciding with archaeal-driven nitrogen metabolism. Morphological observations of the wood fall showed that the SWCS had degraded into a wooden core, whereas the TR and SDCS retained sapwood and intact wooden structures, respectively (Fig. 1c and d). Thus, the TR and SDCS represented the early to middle stages of wood degradation, while the SWCS was in the late stage. Non-uniform degradation levels across sections or interfaces of deep-sea wood falls (e.g., Douglas fir) have been previously reported (Pop Ristova et al., 2017), attributed to distinct aerobic (e.g., SWCS) or anaerobic (e.g., SDCS) environmental conditions at different wood interfaces. Furthermore, archaeal methanogenesis may be spatially and temporally separated from sulfate reducers (Reeburgh and Heggie, 1977)—a pattern likely linked to competition for common substrates within the wood fall (Abram and Nedwell, 1978; Winfrey and Zeikus, 1977). This inference is supported by the functional potential of archaeal communities in the SWCS and SDCS observed in this study. Fagervold et al. (2012) found that sulfate-reducing bacteria exhibited stronger H_2-oxidizing capacity than methanogens, as sulfate concentrations in wood falls exceeded those of formic acid or acetic acid (Fagervold et al., 2012; Yanagawa et al., 2012). During the sulfophilic stage, hydrogen sulfide accumulates at the top surface or SWCS of wood falls. Consequently, in the late stages of wood degradation, methanogenic archaea face more intense substrate competition from sulfate-reducing bacteria—this may explain why archaeal methane metabolism was only detected in the TR and SDCS. Consistent with this, no methanogenic potential was identified in the late degradation stages (121, 240, and 307 days) of experimental pine and oak wood falls; only 16S rRNA gene sequences of ammonia-oxidizing Thaumarchaeota were detected (Kalenitchenko et al., 2015). While sulfate reducers, methanogens, and sulfide oxidizers co-occur in deep-sea wood falls of the Pacific and Mediterranean (Fagervold et al., 2012), this may be associated with the simple structure and small size (0.0003-0.5906 m^2) of these wood falls, which likely fail to provide sufficient substrates and diverse habitats for microorganisms.

Notably, the functional core zone of archaeal nitrogen metabolism was localized in the SWCS (the top of the deep-sea wood fall). Archaeal anaerobic ammonia oxidation (TR: 17.2%; SWCS: 50.0%) and nitrification (TR: 17.1%; SWCS: 50.0%) were active in both the SWCS and TR (Fig. 7c), indicating that archaea serve as primary contributors to the microbial-driven nitrogen cycle in deep-sea wood fall ecosystems.

Previous studies have reported that wood contains 0.08%-0.2% nitrogen (Filipiak, 2018; Meerts, 2002)—far lower than its carbon and sulfide content. As a result, most deep-sea benthic or opportunistic fauna cannot acquire nitrogen directly from wood falls (Harbour et al., 2021a); instead, endosymbiotic microorganisms provide nitrogenase to these fauna, supplementing their nitrogen-deficient diets. For example, *Teredinibacter turnerae* establishes symbioses with marine wood-boring bivalves of the family Teredinidae and plays a key role in urea transport and metabolism in the host (Yang et al., 2009). It was worth noting that microorganism-fauna symbiosis-associated nitrogen cycling appears to be most active during the initial stages of wood degradation, as fauna are scarce in the senescent stage of wood fall ecosystems (Pop Ristova et al., 2017). In contrast, abundant archaea are typically detected in highly degraded wood falls (Palacios et al., 2009). Kalenitchenko et al. (2015) found that sequences of marine group I Thaumarchaeota (genus Nitrospumilus) were abundant at the top of the SWCS in experimental wood falls after 78 days. Nitrospumilus is widely distributed in seawater and capable of oxidizing ammonia to nitrite (Ahlgren et al., 2019; Walker et al., 2010). In this study, archaeal nitrogen metabolism was only detected at the top of the deep-sea wood fall, where the wood bark was completely degraded in the TR and SWCS (Fig. 1c). Thus, we hypothesize that archaea play a key role in nitrogen cycling during the late stages of wood degradation, potentially providing electron acceptors (e.g., nitrate or nitrite) to sulfate-reducing bacteria and promoting sulfide reoxidation. In deep-sea wood falls, monosaccharides produced by the anaerobic degradation of organic matter (e.g., cellulose and lignin) are fermented into small carbon molecules by marine fungi (Pointing et al., 1998; Raghukumar et al., 1994). These small carbon molecules are then reduced by sulfate-reducing bacteria, ultimately producing sulfides. Intermediate products of archaeal-driven nitrogen cycling (e.g., nitrate or nitrite) may serve as electron acceptors for sulfide reoxidation (Kalenitchenko et al., 2015; Muller et al., 2010).

Collectively, archaeal communities play a crucial role in both the carbon-hydrogen and nitrogen cycles of deep-sea wood fall. Archaeal methane and nitrogen metabolism are closely linked to degradation levels across distinct wood interfaces. The weaker substrate competitiveness of methanogenic archaea compared to sulfate-reducing bacteria likely explains why archaeal methane metabolism was only detected in the TR and SDCS (regions with slow degradation rates). In contrast, archaeal nitrogen metabolism may provide essential electron acceptors for sulfate-reducing bacterial sulfide reoxidation, supporting the persistence of archaeal nitrogen metabolism in the SWCS (a region with fast degradation rates).

5. Conclusion

Morphological characterization identified the deep-sea wood fall in this study as *Homalium hainanense* Gagnep.—a key material historically utilized in traditional wooden shipbuilding during the 1970s-1980s. Based on ^{14}C dating, the formation timeframe of the *H. hainanense* wood fall deposit coincides with this period, indicating that the source of this deep-sea wood fall is likely closely associated with post-1970s wooden vessels. Furthermore, the archaeal community's diversity and interaction hub are localized in the TR, which exhibits higher α-diversity, functional diversity, and net immigration rate, as well as resilience, and energy-information transfer efficiency of the AEIN compared to the SDCS and SWCS. The diversity and ecological interaction network center of archaeal community potentially indicate the zone of fastest degradation in deep-sea wood fall, and the dispersal process may contribute to the formation of this hub. TR also may provide a diverse ecological niches for maintenance of unstable archaeal community in deep-sea wood fall. Archaeal community assembly in deep-sea wood fall is dominated by stochastic processes, accounting for over 90% of assembly dynamics across all contact surfaces; these processes likely play a pivotal role in sustaining archaeal diversity. Notably, the TR archaeal community exhibits diverse assembly patterns, suggesting that microhabitat complexity promotes heterogeneous archaeal community assembly trajectories in deep-sea wood fall. Moreover, the ecological functions of the TR archaeal community are co-dominated by methane metabolism (65.7%) and nitrogen metabolism (34.3%). In contrast, SDCS and SWCS are enriched in methane metabolism (97.6%) and nitrogen metabolism (100%), respectively. Consequently, the relative abundances of methane and nitrogen metabolic functional profiles in the archaeal community are closely correlated with the degradation stage of deep-sea wood fall: methane metabolism is active in the archaeal community during the early and middle stages of wood-fall degradation, whereas nitrogen metabolism dominates the community's biogeochemical activities in the late stage. This pattern can be attributed to niche differentiation and changes in the intensity of substrate competition within the archaeal community across different stages of wood-fall degradation. This study highlights the community dynamics, interactions, and functional traits of archaeal microbiota across distinct contact surfaces in deep-sea wood fall in the SCS. These findings provide new insights into the diversity, ecological functions, and biogeochemical processes of prokaryotic wood fall ecosystems in the deep sea.

CRediT authorship contribution statement

Biao Chen: Writing – review & editing, Visualization, Validation, Resources, Methodology, Data curation, Conceptualization. **Xinrui Zhang:** Validation, Resources, Methodology. **Kefu Yu:** Writing – review & editing, Validation, Resources, Project administration, Methodology, Funding acquisition, Conceptualization. **Zeming Bao:** Writing – review & editing, Validation, Methodology, Investigation. **Xinyue Liang:** Validation, Methodology, Investigation. **Xuanlin Li:** Validation, Methodology, Investigation. **Lin Liang:** Validation, Methodology, Investigation. **Qicheng Wu:** Writing – review & editing, Visualization, Validation, Resources, Data curation. **He Li:** Resources, Methodology, Investigation. **Lijia Xu:** Supervision, Resources, Funding acquisition.

Data availability

The raw sequencing datasets of archaeal 16S rRNA amplicons have been deposited in the NCBI Sequence Read Archive (Accession number: PRJNA1221359).

Declaration of competing interest

The authors declare that they have no competing interests.

Acknowledgements

This work was supported by the National Natural Science Foundation of China [No. 42306165]; the Guangxi Science and Technology Program [No. AD25069075]; the National Natural Science Foundation of China [No. 42676151]; the Guangxi Natural Science Foundation [No. 2024GXNSFBA010307]; Guangdong Science and Technology Programme [No.2024B1212050012]; the Central Public-Interest Scientific Institution Basal Research Fund [Nos. PM-zx703-202506-180, PM-zx703-202408-288 and PM-zx703-202506-206]; Innovation and Entrepreneurship Training Program for College Students [No. 202210593089].

References

Abram, J.W., Nedwell, D.B., 1978. Hydrogen as a substrate for methanogenesis and sulphate reduction in anaerobic saltmarsh sediment. Arch. Microbiol. 117 (1), 93–97. https://doi.org/10.1007/BF00689357.

Ahlgren, N.A., Fuchsman, C.A., Rocap, G., Fuhrman, J.A., 2019. Discovery of several novel, widespread, and ecologically distinct marine Thaumarchaeota viruses that encode amoC nitrification genes. ISME J. 13 (3), 618–631. https://doi.org/10.1038/s41396-018-0289-4.

Allen, R., Hoffmann, L.J., Larcombe, M.J., Louisson, Z., Summerfield, T.C., 2020. Homogeneous environmental selection dominates microbial community assembly in

the oligotrophic South Pacific Gyre. Mol. Ecol. 29 (23), 4680–4691. https://doi.org/10.1111/mec.15651.
Amon, D.J., Hilario, A., Arbizu, P.M., Smith, C.R., 2017. Observations of organic falls from the abyssal clarion-clipperton zone in the tropical eastern Pacific Ocean. Mar. Biodivers. 47 (2), 311–321. https://doi.org/10.1007/s12526-016-0572-4.
Bao, Z., Chen, B., Yu, K., Wei, Y., Liang, X., Yao, H., Liao, X., Xie, W., Yin, K., 2025. Microbiome dynamics and functional profiles in deep-sea wood-fall micro-ecosystem: insights into drive pattern of community assembly, biogeochemical processes, and lignocellulose degradation. Appl. Environ. Microbiol. 91 (1), e02124–e02165. https://doi.org/10.1128/aem.02165-24.
Benjamini, Y., Hochberg, Y., 1995. Controlling the false discovery rate: a practical and powerful approach to multiple testing. J. R. Stat. Soc. B, Methodol. 57 (1), 289–300. https://doi.org/10.1111/j.2517-6161.1995.tb02031.x.
Bertolaso, L., Garilli, V., Parrinello, D., Sosso, M., Dell Angelo, B., 2015. A new Miocene deep-sea chiton and early evidence for Teredinidae-sustained wood-fall communities. Palaeontol. Electron. 18 (2), 41A.
Bienhold, C., Pop, R.P., Wenzhofer, F., Dittmar, T., Boetius, A., 2013. How deep-sea wood falls sustain chemosynthetic life. PLoS One 8 (1), e53590. https://doi.org/10.1371/journal.pone.0053590.
Bokulich, N.A., Kaehler, B.D., Rideout, J.R., Dillon, M., Bolyen, E., Knight, R., Huttley, G. A., Gregory Caporaso, J., 2018. Optimizing taxonomic classification of marker-gene amplicon sequences with QIIME 2's q2-feature-classifier plugin. Microbiome 6 (90). https://doi.org/10.1186/s40168-018-0470-z.
Bolyen, E., Rideout, J.R., Dillon, M.R., Bokulich, N.A., Caporaso, J.G., 2019. Author correction: reproducible, interactive, scalable and extensible microbiome data science using QIIME 2. Nat. Biotechnol. 37 (9). https://doi.org/10.1038/s41587-019-0252-6.
Bronk Ramsey, C., 2009. Bayesian analysis of radiocarbon dates. Radiocarbon 51 (1), 337–360. https://doi.org/10.1017/S0033822200033865.
Brown, M.B., 1975. 400: a method for combining non-independent, one-sided tests of significance. Biometrics 987–992. https://doi.org/10.2307/2529826.
Callahan, B.J., Mcmurdie, P.J., Rosen, M.J., Han, A.W., Johnson, A.J.A., Holmes, S.P., 2016. DADA2: high-resolution sample inference from illumina amplicon data. Nat. Methods 13 (7), 581–583. https://coi.org/10.1038/nmeth.3869.
Chase, J.M., 2010. Stochastic community assembly causes higher biodiversity in more productive environments. Science 328 (5984), 1388–1391. https://doi.org/10.1126/science.1187820.
Chen, J., Yang, J., Liu, P., 1992. Compendium of Chinese Woods. China Forestry Publishing House, Beijing.
Cunha, M.R., Matos, F.L., Génio, L., Hilário, A., Moura, C.J., Ravara, A., Rodrigues, C.F., 2013. Are organic falls bridging reduced environments in the deep sea? - results from colonization experiments in the Gulf of Cádiz. PLoS One 8 (10), e76688. https://doi.org/10.1371/journal.pone.0076688.
Deng, Y., Jiang, Y.H., Yang, Y., He, Z., Luo, F., Zhou, J., 2012. Molecular ecological network analyses. BMC Bioinf. 13, 113. https://doi.org/10.1186/1471-2105-13-113.
Distel, D.L., Baco, A.R., Chuang, E., Morrill, W., Cavanaugh, C., Smith, C.R., 2000. Do mussels take wooden steps to deep-sea vents? Nature 403 (6771), 725–726. https://doi.org/10.1038/35001667.
Distel, D.L., Morrill, W., Maclaren-Toussaint, N., Franks, D., Waterbury, J., 2002. Teredinibacter turnerae gen. nov., sp. Nov., a dinitrogen-fixing, cellulolytic, endosymbiotic gamma-proteobacterium isolated from the gills of wood-boring molluscs (Bivalvia: Teredinidae). Int. J. Syst. Evol. Microbiol. 52 (6), 2261–2269. https://doi.org/10.1099/00207713-52-6-2261.
Dubilier, N., Bergin, C., Lott, C., 2008. Symbiotic diversity in marine animals: the art of harnessing chemosynthesis. Nat. Rev. Microbiol. 6 (10), 725–740. https://doi.org/10.1038/nrmicro1992.
Estrada-Peña, A., Cabezas-Cruz, A., Pollet, T., Vayssier-Taussat, M., Cosson, J., 2018. High throughput sequencing and network analysis disentangle the microbial communities of ticks and hosts within and between ecosystems. Front. Cell. Infect. Microbiol. 8. https://doi.org/10.3389/fcimb.2018.00236.
Fagervold, S.K., Galand, P.E., Zbinden, M., Gaill, F., Lebaron, P., Palacios, C., 2012. Sunken woods on the ocean floor provide diverse specialized habitats for microorganisms. FEMS Microbiol. Ecol. 82 (3), 616–628. https://doi.org/10.1111/j.1574-6941.2012.01432.
Faust, K., Raes, J., 2012. Microbial interactions: from networks to models. Nat. Rev. Microbiol. 10 (8), 538–550. https://doi.org/10.1038/nrmicro2832.
Filipiak, M., 2018. Nutrient dynamics in decomposing dead wood in the context of wood eater requirements: the ecological stoichiometry of saproxylophagous insects. In: Ulyshen, M. (Ed.), Saproxylic Insects, Zoological Monographs, vol. 1. Springer, Cham, pp. 429–469. https://doi.org/10.1007/978-3-319-75937-1_13.
Freeman, L.C., 1977. A set of measures of centrality based on betweenness. Sociometry 40 (1), 35–41. https://doi.org/10.2307/3033543.
Gregory, D., Jensen, P., 2006. The importance of analysing waterlogged wooden artefacts and environmental conditions when considering their in situ preservation. J. Wetl. Archaeol. 6 (1), 65–81. https://doi.org/10.1179/jwa.2006.6.1.65. http://www.tandfonline.com/doi/full/10.1179/jwa.2006.6.1.65. (Accessed 18 July 2013).
Harbour, R.P., Smith, C.R., Fernandes, T.F., Sweetman, A.K., 2021a. Trophic ecology surrounding kelp and wood falls in deep Norwegian fjords. Deep-Sea Res. Pt. I 173, 103553. https://doi.org/10.1016/j.dsr.2021.103553.
Harbour, R.P., Smith, C.R., Simon-Nutbrown, C., Cecchetto, M., Young, E., Coral, C., Sweetman, A.K., 2021b. Biodiversity, community structure and ecosystem function on kelp and wood falls in the Norwegian deep sea. Mar. Ecol. Prog. Ser. 657, 73–91. https://www.jstor.org/stable/26988395.
Hua, Q., Barbetti, M., Rakowski, A.Z., 2013. Atmospheric radiocarbon for the period 1950-2010. Radiocarbon 55 (4), 2059–2072. https://doi.org/10.2458/azu_js_rc.v55i2.16177.
Jaillard, B., Rapaport, A., Harmand, J., Brauman, A., Nunan, N., 2014. Community assembly effects shape the biodiversity-ecosystem functioning relationships. Funct. Ecol. 28 (6), 1523–1533. https://doi.org/10.1111/1365-2435.12267.
Jiao, C., Zhao, D., Zeng, J., Guo, L., Yu, Z., 2020. Disentangling the seasonal co-occurrence patterns and ecological stochasticity of planktonic and benthic bacterial communities within multiple lakes. Sci. Total Environ. 740, 140010. https://doi.org/10.1016/j.scitotenv.2020.140010.
Jørgensen, B.B., Boetius, A., 2007. Feast and famine-microbial life in the deep-sea bed. Nat. Rev. Microbiol. 5 (10), 770–781. https://doi.org/10.1038/nrmicro1745.
Judge, J., Barry, J.P., 2016. Macroinvertebrate community assembly on deep-sea wood falls in monterey bay is strongly influenced by wood type. Ecology 97 (11), 3031–3043. https://doi.org/10.1002/ecy.1546.
Kalenitchenko, D., Fagervold, S.K., Pruski, A.M., Vetion, G., Yucel, M., Le Bris, N., Galand, P.E., 2015. Temporal and spatial constraints on community assembly during microbial colonization of wood in seawater. ISME J. 9 (12), 2657–2670. https://doi.org/10.1038/ismej.2015.61.
Kiel, S., Amano, K., Hikida, Y., Jenkins, R.G., 2009. Wood-fall associations from Late Cretaceous deep-water sediments of Hokkaido, Japan. Lethaia 42 (1), 74–82. https://doi.org/10.1111/j.1502-3931.2008.00105.x.
Knights, D., Kuczynski, J., Charlson, E.S., Zaneveld, J., Mozer, M.C., Collman, R.G., Bushman, F.D., Knight, R., Kelley, S.T., 2011. Bayesian community-wide culture-independent microbial source tracking. Nat. Methods 8 (9). https://doi.org/10.1038/nmeth.1650, 761-U107.
Li, Q., Liu, Y., Li, G., Wang, Z., Zheng, Z., Sun, Y., Lei, N., Li, Q., Zhang, W., 2022. Review of the impact of whale fall on biodiversity in deep-sea ecosystems. Front. Ecol. Evol. 10, 885572. https://doi.org/10.3389/fevo.2022.885572.
Li, Y., 2009. Hainan Provincial records-fisheries Records. Nanhai Publishing Company, Haikou.
Lima, L.F.O., Weissman, M., Reed, M., Papudeshi, B., Alker, A.T., Morris, M.M., Edwards, R.A., de Putron, S.J., Vaidya, N.K., Dinsdale, E.A., 2020. Modeling of the coral microbiome: the influence of temperature and microbial network. mBio 11 (2). https://doi.org/10.1128/mbio.02691-19 e02691-19.
Liu, C., Li, H., Zhang, Y., Si, D., Chen, Q., 2016. Evolution of microbial community along with increasing solid concentration during high-solids anaerobic digestion of sewage sludge. Bioresour. Technol. 216, 87–94. https://doi.org/10.1016/j.biortech.2016.05.048.
Liu, S., Yu, H., Yu, Y., Huang, J., Zhou, Z., Zeng, J., Chen, P., Xiao, F., He, Z., Yan, Q., 2022. Ecological stability of microbial communities in Lake Donghu regulated by keystone taxa. Ecol. Indic. 136, 108695. https://doi.org/10.1016/j.ecolind.2022.108695.
Louca, S., Parfrey, L.W., Doebeli, M., 2016. Decoupling function and taxonomy in the global ocean microbiome. Science 353 (6305), 1272–1277. https://doi.org/10.1126/science.aaf4507.
Ma, B., Wang, H., Dsouza, M., Lou, J., He, Y., Dai, Z., Brookes, P.C., Xu, J., Gilbert, J.A., 2016. Geographic patterns of co-occurrence network topological features for soil microbiota at continental scale in eastern China. ISME J. 10 (8), 1891–1901. https://doi.org/10.1038/ismej.2015.261.
Martin, W., Baross, J., Kelley, D., Russell, M.J., 2008. Hydrothermal vents and the origin of life. Nat. Rev. Microbiol. 6 (11), 805–814. https://doi.org/10.1038/nrmicro1991.
Matthiesen, H., Jensen, J.B., Gregory, D., Hollesen, J., Elberling, B., 2014. Degradation of archaeological wood under freezing and thawing conditions-effects of permafrost and climate change. Archaeometry 56 (3), 479–495. https://doi.org/10.1111/arcm.12023.
Meerts, P., 2002. Mineral nutrient concentrations in sapwood and heartwood: a literature review. Ann. Sci. 59 (7), 713–722. https://doi.org/10.1051/forest:2002059.
Moseley, R.D., Hampel, J.J., Mugge, R.L., Hamdan, L.J., 2022. Historic wooden shipwrecks influence dispersal of deep-sea biofilms. Front. Mar. Sci. 9, 873445. https://doi.org/10.3389/fmars.2022.873445.
Muller, F., Brissac, T., Le Bris, N., Felbeck, H., Gros, O., 2010. First description of giant Archaea (thaumarchaeota) associated with putative bacterial ectosymbionts in a sulfidic marine habitat. Environ. Microbiol. 12 (8), 2371–2383. https://doi.org/10.1111/j.1462-2920.2010.02309.x.
Nemergut, D.R., Schmidt, S.K., Fukami, T., O'Neill, S.P., Bilinski, T.M., Stanish, L.F., Knelman, J.E., Darcy, J.L., Lynch, R.C., Wickey, P., Ferrenberg, S., 2013. Patterns and processes of microbial community assembly. Microbiol. Mol. Biol. Rev. 77 (3), 342–356. https://doi.org/10.1128/MMBR.00051-12.
Oksanen, J., Blanchet, F.G., Kindt, R., 2015. Vegan: commity ecology package. R Package Version 2, 3-0.
Olsson, I.U., 1980. 14C in extractives from wood. Radiocarbon 22 (2), 515–524. https://doi.org/10.1017/S0033822200009838.
Palacios, C., Zbinden, M., Pailleret, M., Gaill, F., Lebaron, P., 2009. Highly similar prokaryotic communities of sunken wood at shallow and deep-sea sites across the oceans. Microb. Ecol. 58 (4), 737–752. https://doi.org/10.1007/s00248-009-9538-4.
Pereira, O.S., Gonzalez, J., Mendoza, G., Le, J., Mcneill, M., Ontiveros, J., Lee, R.W., Rouse, G.W., Cortés, J., Levin, L.A., 2022. Does substrate matter in the deep sea? A comparison of bone, wood, and carbonate rock colonizers. PLoS One 17 (7), e0271635. https://doi.org/10.1371/journal.pone.0271635.
Pereira, O.S., Shimabukuro, M., Bernardino, A.F., Sumida, P.Y., 2020. Molecular affinity of southwest Atlantic Alvinocaris muricola with Atlantic equatorial belt populations. Deep-Sea Res. Pt. I 163, 103343. https://doi.org/10.1016/j.dsr.2020.103343.
Pires, A.C.C., Cleary, D.F.R., Almeida, A., Cunha, Â., Dealtry, S., Mendonça-Hagler, L.C. S., Smalla, K., Gomes, N.C.M., 2012. Denaturing gradient gel electrophoresis and

barcoded pyrosequencing reveal unprecedented archaeal diversity in mangrove sediment and rhizosphere samples. Appl. Environ. Microbiol. 78, 5520–5528. https://doi.org/10.1128/AEM.00386-12.

Pointing, S.B., Vrijmoed, L., Jones, E., 1998. A qualitative assessment of lignocellulose degrading enzyme activity in marine fungi. Bot. Mar. 41 (3), 293–298. https://doi.org/10.1515/botm.1998.41.1-6.293.

Pop Ristova, P., Bienhold, C., Wenzhöfer, F., Rossel, P.E., Boetius, A., 2017. Temporal and spatial variations of bacterial and faunal communities associated with deep-sea wood falls. PLoS One 12 (1), e0169906. https://doi.org/10.1371/journal.pone.0169906.

Raghukumar, C., Raghukumar, S., Chinnaraj, A., Chandramohan, D., D'Souza, T., Reddy, C., 1994. Laccase and other lignocellulose modifying enzymes of marine fungi isolated from the Coast of India. Bot. Mar. (37), 515–542. https://doi.org/10.1515/botm.1994.37.6.515.

Reeburgh, W.S., Heggie, D.T., 1977. Microbial methane consumption reactions and their effect on methane distributions in freshwater and marine environments. Limnol. Oceanogr. 22 (1), 1–9. https://doi.org/10.4319/lo.1977.22.1.0001.

Reimer, P.J., Bard, E., Bayliss, A., Beck, J.W., Blackwell, P.G., Ramsey, C.B., Buck, C.E., Cheng, H., Edwards, R.L., Friedrich, M., Grootes, P.M., Guilderson, T.P., Haflidason, H., Hajdas, I., Hatté, C., Heaton, T.J., Hoffmann, D.L., Hogg, A.G., Hughen, K.A., Kaiser, K.F., Kromer, B., Manning, S.W., Niu, M., Reimer, R.W., Richards, D.A., Scott, E.M., Southon, J.R., Staff, R.A., Turney, C.S.M., van der Plicht, J., 2013. IntCal13 and Marine13 radiocarbon age calibration curves 0-50,000 years cal BP. Radiocarbon 55 (4), 1869–1887. https://doi.org/10.2458/azu_js_rc.55.16947.

Shannon, P., Markiel, A., Ozier, O., Baliga, N.S., Wang, J.T., Ramage, D., Amin, N., Schwikowski, B., Ideker, T., 2003. Cytoscape: a software environment for integrated models of biomolecular interaction networks. Genome Res. 13 (11), 2498–2504. https://doi.org/10.1101/gr.1239303.

Stewart, F.J., Newton, I.L., Cavanaugh, C.M., 2005. Chemosynthetic endosymbioses: adaptations to oxic-anoxic interfaces. Trends Microbiol. 13 (9), 439–448. https://doi.org/10.1016/j.tim.2005.07.007.

Tandberg, A.H.S., Rapp, H.T., Schander, C., Vader, W., 2013. A new species of exitomelita (Amphipoda: melitidae) from a deep-water wood fall in thenorthern Norwegian Sea. J. Nat. Hist. 47 (25–28), 1875–1889. https://doi.org/10.1080/00222933.2012.725778.

Voight, J.R., 2015. Xylotrophic bivalves: aspects of their biology and the impacts of humans. J. Molluscan Stud. 81 (2), 175–186. https://doi.org/10.1093/mollus/eyv008.

Wagg, C., Bender, S.F., Widmer, F., van der Heijden, M., 2014. Soil biodiversity and soil community composition determine ecosystem multifunctionality. Proc. Natl. Acad. Sci. USA 111 (14), 5266–5270. https://doi.org/10.1073/pnas.1320054111.

Walker, C.B., de la Torre, J.R., Klotz, M.G., Urakawa, H., Pinel, N., Arp, D.J., Brochier-Armanet, C., Chain, P.S.G., Chan, P.P., Gollabgir, A., Hemp, J., Hügler, M., Karr, E. A., Könneke, M., Shin, M., Lawton, T.J., Lowe, T., Martens-Habbena, W., Sayavedra-Soto, L.A., Lang, D., Sievert, S.M., Rosenzweig, A.C., Manning, G., Stahl, D.A., 2010. Nitrosopumilus maritimus genome reveals unique mechanisms for nitrification and autotrophy in globally distributed marine crenarchaea. Proc. Natl. Acad. Sci. USA 107 (19), 8818–8823. https://doi.org/10.1073/pnas.0913533107.

Waterbury, J.B., Calloway, C.B., Turner, R.D., 1983. A cellulolytic nitrogen-fixing bacterium cultured from the gland of deshayes in shipworms (Bivalvia: Teredinidae). Science 221 (4618), 1401–1403. https://doi.org/10.1016/j.palwor.2025.200987.

Wen, T., Xie, P., Penton, C.R., Hale, L., Thomashow, L.S., Yang, S., Ding, Z., Su, Y., Yuan, J., Shen, Q., 2022. Specific metabolites drive the deterministic assembly of diseased rhizosphere microbiome through weakening microbial degradation of autotoxin. Microbiome 10 (1), 177. https://doi.org/10.1186/s40168-022-01375-z.

Winfrey, M.R., Zeikus, J.G., 1977. Effect of sulfate on carbon and electron flow during microbial methanogenesis in freshwater sediments. Appl. Environ. Microbiol. 33 (2), 275–281. https://doi.org/10.1128/aem.33.2.275-281.1977.

Wolff, T., 1979. Magrofaunal utilization of plant remains in the deep sea. Sarsia 64 (1–2), 117–143. https://doi.org/10.1080/00364827.1979.10411373.

Xun, W., Liu, Y., Li, W., Ren, Y., Xiong, W., Xu, Z., Zhang, N., Miao, Y., Shen, Q., Zhang, R., 2021. Specialized metabolic functions of keystone taxa sustain soil microbiome stability. Microbiome 9 (1), 35. https://doi.org/10.1186/s40168-020-00985-9.

Yanagawa, K., Matsumoto, R., Suzuki, Y., 2012. Subseafloor biosphere mediating global methane cycle. J. Japt. 77 (5), 374–383. https://doi.org/10.3720/japt.77.374.

Yang, J.C., Madupu, R., Durkin, A.S., Ekborg, N.A., Pedamallu, C.S., Hostetler, J.B., Radune, D., Toms, B.S., Henrissat, B., Coutinho, P.M., 2009. The complete genome of Teredinibacter turnerae T7901: an intracellular endosymbiont of marine wood-boring bivalves (shipworms). PLoS One 4 (7), e6085. https://doi.org/10.1371/journal.pone.0006085.

Yao, X., 1988. Structure of Major Chinese Woods: Scanning Electron Microscope. China Forestry Publishing House, Beijing.

Yuan, M.M., Guo, X., Wu, L., Zhang, Y., Xiao, N., Ning, D., Shi, Z., Zhou, X., Wu, L., Yang, Y., Tiedje, J.M., Zhou, J., 2021. Climate warming enhances microbial network complexity and stability. Nat. lim. Chang. 11 (4), 343–348. https://doi.org/10.1038/s41558-021-00989-9.

Zhang, B., Ning, D., Yang, Y., Van Nostrand, J.D., Zhou, J., Wen, X., 2020. Biodegradability of wastewater determines microbial assembly mechanisms in full-scale wastewater treatment plants. Water Res. 169, 115276. https://doi.org/10.1016/j.watres.2019.115276.

Zhou, J., Deng, Y., Luo, F., He, Z., Tu, Q., Zhi, X., 2010. Functional molecular ecological networks. mBio 1 (4). https://doi.org/10.1128/mBio.00169-10 e00169-10.

Zhou, J., Ning, D., 2017. Stochastic community assembly: does it matter in microbial ecology? Microbiol. Mol. Biol. Rev. 81 (4). https://doi.org/10.1128/mmbr.00002-17 e00002-17.